

# CHEMISTRY

## A European Journal

A Journal of



### Accepted Article

**Title:** Double sequential encrypted targeting sequence: A new concept for bone cancer treatment

**Authors:** Gonzalo Villaverde, Valentina Nairi, Alejandro Baeza, and Maria Vallet-Regi

This manuscript has been accepted after peer review and appears as an Accepted Article online prior to editing, proofing, and formal publication of the final Version of Record (VoR). This work is currently citable by using the Digital Object Identifier (DOI) given below. The VoR will be published online in Early View as soon as possible and may be different to this Accepted Article as a result of editing. Readers should obtain the VoR from the journal website shown below when it is published to ensure accuracy of information. The authors are responsible for the content of this Accepted Article.

**To be cited as:** *Chem. Eur. J.* 10.1002/chem.201605947

**Link to VoR:** <http://dx.doi.org/10.1002/chem.201605947>

Supported by  
**ACES**

WILEY-VCH

## Double sequential encrypted targeting sequence: A new concept for bone cancer treatment.

Gonzalo Villaverde,<sup>[a]</sup> Valentina Nairi,<sup>[a]</sup> Alejandro Baeza,<sup>[a]\*</sup> and María Vallet-Regí.<sup>[a]\*</sup>

In the memory of Prof. José Barluenga Mur

**Abstract:** The selective transportation of therapeutic agents to tumoral cells is usually achieved by their conjugation with targeting moieties able to recognize these cells. Unfortunately, simple and static targeting systems usually show selectivity lacks. Herein, double sequential encrypted targeting system is proposed as stimuli-responsive targeting analogue for selectivity enhancement. The system is able to recognize diseased bone tissue in first place, and once there, a hidden secondary targeting group is activated by the presence of an enzyme overproduced in the malignant tissue (cathepsin K), triggering the recognition of diseased cells. Transporting the cell targeting agent in a hidden conformation which contains a high selective tissular primary targeting, could avoid not only its binding to similar cell receptors but also the apparition of the binding-site barrier effect, which can enhance the penetration of the therapeutic agent within the affected zone. This strategy could be applied not only to conjugate drugs but also to drug loaded nanocarriers in order to improve the efficiency for bone cancer treatments.

The selectivity lack of cytotoxic drugs results in an ineffective delivery of them in tumoral tissues, which strongly reduces their efficacy and causes the apparition of systemic toxicity in usual cancer treatments.<sup>[1]</sup> Moreover, even if the drug reaches the tumoral area, it should be face a complex scenario. A solid tumor is an extraordinary heterogeneous tissue formed by myriad of different malignant, harmless, even supportive cells, which play different roles in tumor progression.<sup>[2]</sup> Therefore, it is necessary to design smart therapeutic agents with the ability to distinguish between healthy and tumoral cells in order to enhance their efficiency through the concentration of their cytotoxic capacity exclusively in malignant cells. One of the promising alternatives for improving the selectivity of chemotherapy is the covalent conjugation of vectorization moieties or targeting systems, directly on the surface of drug-loaded nanocarriers,<sup>[3]</sup> with both inorganic<sup>[4],[5]</sup> and organic nature,<sup>[6],[7]</sup> as well as, with the own free drugs<sup>[8]</sup> generating vectorized drug conjugates. There are a wide variety of targeting systems, from big biomolecules as antibodies,<sup>[9]</sup> lipoproteins<sup>[10]</sup>

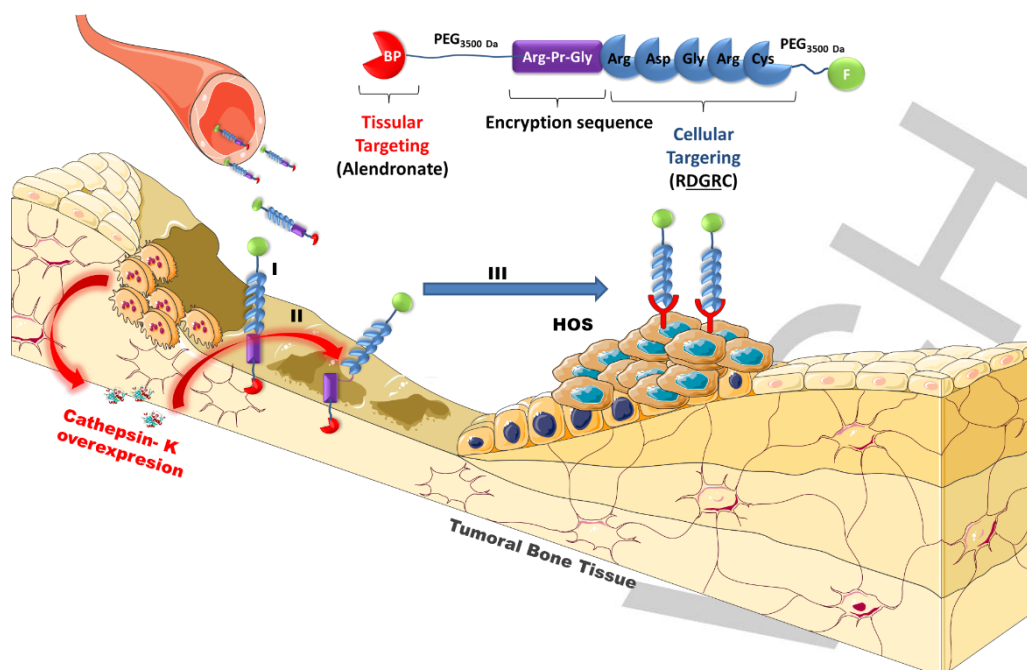
or oligonucleotide sequences<sup>[11]</sup> to small molecules such as vitamins,<sup>[12]</sup> sugars<sup>[13]</sup> or synthetic molecules.<sup>[14]</sup> These moieties are characterized by their capacity to recognize and specifically bind to membrane cell receptors which are only, or mainly expressed by tumoral cells. Unfortunately, the use of targeting moieties is not free of drawbacks presenting some unwanted effects as off-target by protein corona<sup>[15]</sup> or non-desired modifications in the ligand during the conjugation process,<sup>[16]</sup> besides the cross interactions between the targeting group and cell receptors expressed in healthy cells. On the other hand, strong binding affinity between the vectorization motif and its cell receptor severely hampers the penetration of the therapeutic agent within the tumor. The apparition of this well-known effect, called binding-site barrier, is common in both, drug conjugates<sup>[17]</sup> and targeted nanoparticles<sup>[18]</sup> and compromises the efficacy of the therapy by accumulation of targeted systems mainly in the tumor periphery inducing outside weak local effects.

Hierarchical targeting has been recently proposed as a novel strategy able to overcome these limitations in the case of nanometric carriers.<sup>[19]</sup> However, using shielded targeting agents in this context makes EPR<sup>[20],[21]</sup> effect as solely responsible for nanocarrier accumulation in tumoral tissues.<sup>[22]</sup> Therefore, the achieved gain regarding lower cross interactions and higher penetration could be counteracted by the lower amount of nanocarriers which reach the diseased zone. Additionally, this approach is hardly adaptable to the direct conjugation with small drugs, due to these therapeutic agents do not present EPR effect, as a consequence of their smaller size.

Herein, we propose a novel approach equally applicable both drug conjugates and nanocarriers. This concept is based on a double sequential encrypted targeting system (DSETS) capable to combine tissular and cellular targeting following an activatable cascade mechanism. As proof of concept, we have focused on bone tumors. Thereby, we have chosen an uncovered primary tissue targeting agent, bisphosphonate (BP) specific for exposed diseased bone tissue, and secondary hidden cellular targeting "RGD type". The peptide has been encrypted inside an oligopeptide sequence RPGRDGRGRC (Arg-Pr-Gly-Arg-Asp-Gly-Arg-Cys) and has been sterically covered with a polyethyleneglycol 3500 Da, (PEG) moiety, making it more inert in presence of its receptors. Then, the RGD pattern becomes exposed only in the presence of elevated concentrations of cathepsin-K (CK), characteristic behavior of bone tissues with high osteoclast activity such as many primary and metastatic bone tumors <sup>[23],[24]</sup> (**Scheme 1.**) This novel targeting moiety is based on the combination of two widely employed targeting agents as are both; alendronate<sup>[25]</sup> (ALN) and RGD tripeptide.<sup>[26],[27]</sup> Alendronate shows high avidity by hydroxyapatite and therefore, this molecule strongly binds to the mineral part of bone tissues.<sup>[28]</sup>

[a] Prof. María Vallet-Regí and Dr. Alejandro Baeza  
Depto. Química Inorgánica y Bioinorgánica. Facultad de Farmacia,  
Universidad Complutense de Madrid. Plaza Ramon y Cajal s/n.  
Instituto de Investigación Sanitaria Hospital 12 de Octubre i+12 i  
Centro de Investigación Biomédica en Red de Bioingeniería,  
Biomateriales y Nanomedicina (CIBER-BBN)  
Madrid, Spain  
E-mail: [vallet@ucm.es](mailto:vallet@ucm.es); [abaezaga@ucm.es](mailto:abaezaga@ucm.es)

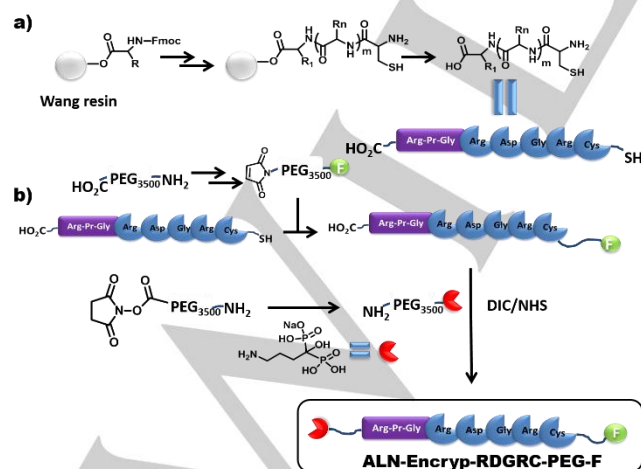
Supporting Information is available from the Wiley Online Library or from the author: synthetic procedures, NMR and MALDI-TOF/TOF spectra, cell culture protocols and flow cytometry measurements.



**Scheme 1.** Mode of action of the double sequential targeting system in osteosarcoma diseased bone. I) Bone fixing HA-BP, II) Cathepsin-K induced peptide proteolysis and III) RGD peptide recognition by HOS cells wall and subsequent internalization.

On the other hand, RGD pattern is a well-known sequence which binds to  $\alpha_v\beta_3$ -integrin and Neuropilin (NRP)-1 receptors which are usually overexpressed in many tumoral cell lines and also in tumoral blood vessels.<sup>[29]</sup>

However, integrin receptors are also present in many healthy cells and therefore, the direct conjugation of RGD sequences on the transported specie could misdirect the therapeutic cargo to unwanted locations. The combination of both vectorization capacities (tissular and cellular targeting) converts this modular targeting system into a promising prototype for delivering therapeutic agents to bone tumors. For affording the targeting device, the first step was the synthesis of the polypeptide strand which was made using solid phase chemistry starting by Fmoc-Arg(Pbf)-Wang resin (see supporting information for the detailed protocol).



**Scheme 2.** Synthetic pathway for affording fluorescent dual-targeting moiety.

Following the typical Fmoc-deprotection and HBTU/HOBT-mediated carboxylic acid activation steps, each aminoacids was introduced in the peptide strand (**Scheme 2a**). The tripeptide Arg-Pr-Gly motif was introduced in the sequence for providing selective responsivity to CK. This enzyme performs the proteolysis of collagen I catalyzing almost exclusively the rupture of the amide bond present in the helix after Pr-Gly motif.<sup>[30],[31]</sup>

In order to evaluate the sensitivity and selectivity against CK, a small amount of the peptide strand (10 mg) was exposed to an acidic solution of this enzyme (pH = 5) during two hours at 37 °C replicating osteoclast lacuna conditions. Whereas, other batch was only exposed to mild acidic medium. After isolation process, the resulted crudes were analyzed by matrix-assisted laser desorption/ionization (MALDI) time-of-flight/time-of-flight (TOF/TOF). As it was expected, when the peptide was exposed to CK, Arg-Asp-Gly-Arg-Cys was the mayor product, as corresponds to the amide bond rupture after glycine in Pr-Gly (Figure S10). This result confirm that CK induces the responsive behavior of the peptide strand in front of the stability showed in enzyme-free conditions. A fluorescent labeled polyethyleneglycol (F-PEG) was employed as therapeutic cargo model. This polymeric strand mimics the role of nanometric drug-loaded carrier or therapeutic macromolecule allowing an easy visualization and quantification of the system internalization within malignant cells, as it has been reported elsewhere.<sup>[32]</sup> F-PEG-Maleimide was attached to the cysteine end through thiol-ene reaction. Alendronate was conjugated via carbodiimide chemistry to the carboxylic acid end of a bifunctional HO<sub>2</sub>C-PEG-NH<sub>2</sub> chain of 3500 Da of molecular weight in order to shield more properly the cellular targeting moiety. Finally, this system was attached on the fluorescent peptide strand using again a carbodiimide, as carboxylic acid activator. (**Scheme 2b**).

Once the system was prepared, its performance was evaluated step by step. Firstly, its capacity to bind apatite was tested by incubating the complete system in the presence of pure hydroxyapatite discs (HA) in PBS, pH=7.4 at 37°C, during 8 hours simulating body fluids conditions. The peptide sequence without PEG-alendronate moiety was employed as control. After this time, the discs were thoroughly washed with buffer in order to eliminate the physically adsorbed systems and their presence was determined by fluorescence microscopy. As it was expected, the peptides without alendronate were not able to bind to the surface of HA discs whereas the peptides with alendronate were strongly retained on HA surface (**Figure 1a**). Further, binding capacity was also evaluated in the presence of  $\text{Ca}^{2+}$  at concentration of 2.5 mM, which is naturally present in bone tissue surrounding. HA discs with complete system was incubated in the presence of physiological concentration of  $\text{Ca}^{2+}$  showing the retention of fluorescence in a similar amount than controls without  $\text{Ca}^{2+}$  (**Figure 1b**). As it is shown in the figure 1b, it was necessary to double this concentration for releasing in a significant amount the targeting moiety.

In order to prove that the binding capacity of the complete system was due to the complexation of alendronate on HA surface, competition experiments with free alendronate were carried out. As is shown in **Figure 1c**, the system ability to be retained on HA surface decreased when alendronate concentration was higher, due to free alendronate was gradually replacing the complete targeting device from the surface. In all experiments, the targeting system release was confirmed by fluorescence measurements of the solutions before and after the alendronate exposition (Graphic S1). In sight of these evidences, the active primary targeting inside the complete system showed a good performance in close reality conditions for vectorization to diseased bone.

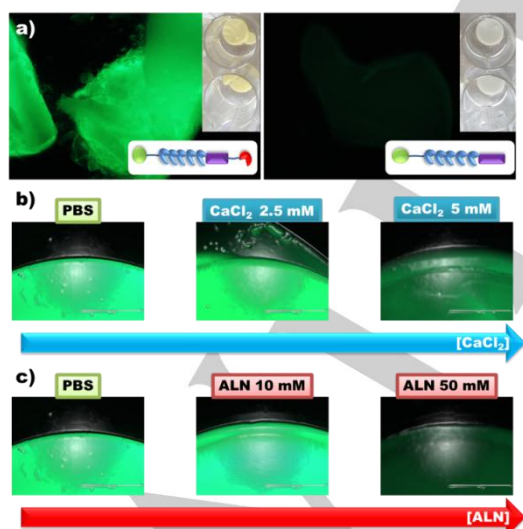


**Figure 1.** a) Fluorescence microscopy HA discs exposed to the targeting device with and without PEG-alendronate. Fluorescence microscopy of HA discs exposed to complete targeting device in the presence of different concentrations of b)  $\text{Ca}^{2+}$  and c) free alendronate.

The next step was to evaluate the performance of the hidden secondary targeting sequence. For this aim, Human Osteosarcoma cells (HOS) was chosen as tumoral cell model because they usually overexpress  $\alpha_v\beta_3$ -integrin<sup>[33]</sup> and (NRP)-1 receptors<sup>[34]</sup> which interact with the RGD pattern. Further, osteosarcoma is one of the most common non-hematologic neoplasm which affects to bone tissues.<sup>[35]</sup> The capacity to hide the secondary targeting was evaluated exposing HOS cells to a fixed concentration of complete system (10  $\mu\text{g}/\text{mL}$ ) during 2 hours. The same protocol was carried out employing a fluorescent PEG strand (F-PEG) as negative control and a fluorescent PEG strand decorated with CRGDR as positive control (F-PEG-CRGDR), respectively. The percentage of cells that internalize the fluorescent strands in each case was measured using flow cytometry. Almost 20% of HOS cells internalize the fragment which contains the unshielded RGD pattern in comparison with only 8% of cells which engulf the fluorescent PEG, which confirm that the RGD sequence enhances the internalization within malignant cells (**Figure 2**). Interestingly, targeting uptake was only 12% (all data normalized with control) when the complete system that contains the shield pattern was employed, which correspond to around 40% of decrease in targeting internalization. Thus, these results point out a good performance of both encryption and cell targeting capacity of the hybrid strand.

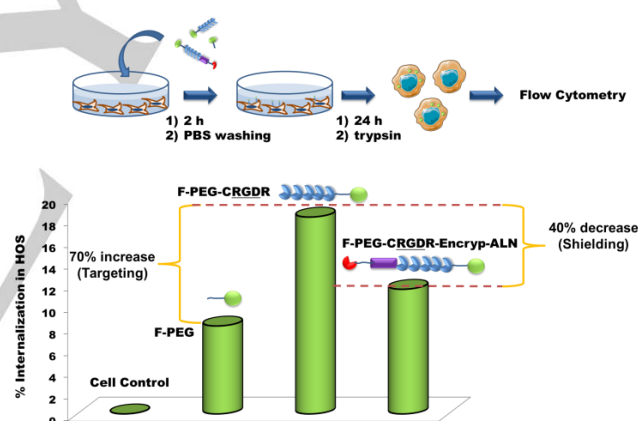


**Figure 2.** Studies of internalization capacity of F-PEG, F-PEG-CRGDR and F-PEG-CRGDR-Encryp-ALN in HOS. Error data and statistical analysis in supporting information.

Finally, the complete system was tested employing a "bone/culture *in vitro* model". In this model, HA discs were previously incubated with PBS solution which contains 300  $\mu\text{g}\cdot\text{mL}^{-1}$  of complete system. After 8 hours, the discs were thoroughly washed with buffer in order to remove the physisorbed peptide. Once the discs were washed, they were placed on upper sheet of transwells and the cells were cultured in the inserts. Then, a solution of CK in mild-acidic media was added to three wells while other three batches were only exposed to the mild-acidic solution without the enzyme and they were incubated during 2 hours. After the incubation time, HA discs were retired and cell cultures were washed with PBS and incubated with medium during 24 hours more.



The targeting internalization in each well were analyzed by flow cytometry showing that, in the samples where cathepsin-K was added, around 90 % of cells showed fluorescence which indicates the internalization of the labeled peptide. On contrary, in the wells incubated without CK, only around 10 % of the cells exhibited fluorescence. The presence of the peptide in each disc was observed by fluorescence microscopy showing that discs which were treated with incubated proteolytic enzyme lost all the fluorescence whereas in those without the enzyme, the fluorescence is almost completely retained (Figure 3).

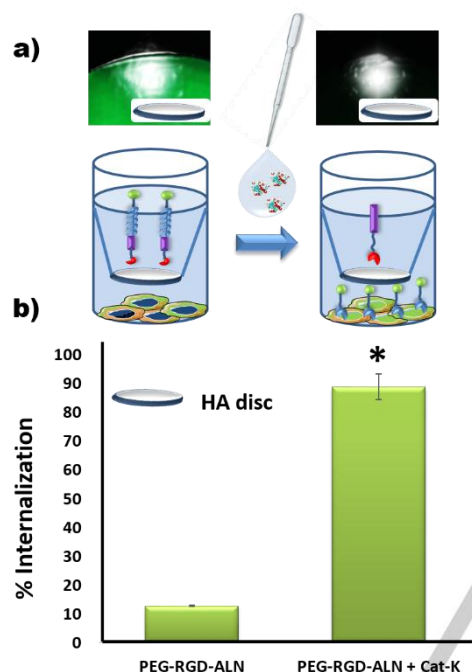


**Figure 3.** Cathepsin-K responsive behavior in HOS before and after CK by a) fluorescence microscopy of HA discs addition, b) percentage of cells which have engulfed the fluorescent label. \*  $P < 0.01$

Osteosarcoma has been chosen as proof of concept of a common solid tumor and therefore, the primary and secondary targeting groups were selected accordingly. But it is worth noting that this strategy could be easily adapted to different tumors which affect to different organs or tissues. In conclusion, encrypted targeting agents would avoid the misdirection of the transported species to other tissues reducing the apparition of side effects or systemic toxicity. Additionally, the primary targeting group located at the end of full system provides the guiding capacity to the affected tissue. This novel targeting system represents a new approach for the selectivity enhancement in drug delivery processes and it could be applied for several types of drug conjugates, drug loaded nanocarriers or imaging agents, increasing the available arsenal in the fight against tumors.

## Acknowledgements

This work was supported by the European Research Council (Advanced Grant VERDI; ERC-2015-AdG Proposal No. 694160) and the project MAT2015-64831-R. The authors want to thanks Prof. Maura Monduzzi for her support along this work. For the elaboration of Figures and Schemes, some templates from <http://www.servier.com/Powerpoint-image-bank> have been used.

**Keywords:** Stimuli-responsive targeting, dual-targeting, nano-oncology, encrypted peptide, osteosarcoma

- [1] K. D. Miller, R. L. Siegel, C. C. Lin, A. B. Mariotto, J. L. Kramer, J. H. Rowland, K. D. Stein, R. Alteri, A. Jemal, *CA. Cancer J. Clin.* **2016**, 66, 271–89.
- [2] M. Egeblad, E. S. Nakasone, Z. Werb, *Dev. Cell* **2010**, 18, 884–901.
- [3] R. Bazak, M. Hour, S. El Achy, S. Kamel, T. Refaat, *J. Cancer Res. Clin. Oncol.* **2014**, 141, 769–784.
- [4] M. Vallet-Regi, A. Rámila, R. P. del Real, J. Pérez-Pariante, *Chem. Mater.* **2001**, 13, 308–311.
- [5] M. Vallet-Regi, F. Balas, D. Arcos, *Angew. Chem. Int. Ed. Engl.* **2007**, 46, 7548–58.
- [6] M. Talelli, M. Barz, C. J. F. Rijcken, F. Kiessling, W. E. Hennink, T. Lammers, *Nano Today* **2015**, 10, 93–117.
- [7] M. C. Parrott, J. C. Luft, J. D. Byrne, J. H. Fain, M. E. Napier, J. M. DeSimone, *J. Am. Chem. Soc.* **2010**, 132, 17928–17932.
- [8] E. L. Sievers, P. D. Senter, *Annu. Rev. Med.* **2013**, 64, 15–29.
- [9] Q. Dai, Y. Yan, C. Ang, K. Kempe, M. M. J. Kamphuis, S. J. Dodds, F. Caruso, *ACS Nano* **2015**, 9, 2876–2885.
- [10] S. Lara, F. Alnasser, E. Polo, D. Garry, M. C. Lo Giudice, D. R. Hristov, L. Rocks, A. Salvati, Y. Yan, K. A. Dawson, *ACS Nano* **2017**, acsnano.6b07933.
- [11] Y. Lao, K. K. L. Phua, K. W. Leong, *ACS Nano* **2015**, 9, 2235–2254.
- [12] H. Elnakat, M. Ratnam, *Adv. Drug Deliv. Rev.* **2004**, 56, 1067–1084.
- [13] H. Nguyen, P. Katavic, N. A. H. Bashah, V. Ferro, *ChemistrySelect* **2016**, 1, 31–35.
- [14] G. Villaverde, A. Baeza, G. J. Melen, A. Alfranca, M. Ramirez, M. Vallet-Regi, *J. Mater. Chem. B* **2015**, 3, 4831–4842.
- [15] A. Salvati, A. S. Pitek, M. P. Monopoli, K. Prapainop, F. B. Bombelli, D. R. Hristov, P. M. Kelly, C. Åberg, E. Mahon, K. A. Dawson, *Nat. Nanotechnol.* **2013**, 8, 137–43.
- [16] L. M. Herda, D. R. Hristov, M. C. Lo Giudice, E. Polo, K. A. Dawson, *J. Am. Chem. Soc.* **2017**, 139, 111–114.
- [17] R. Bakhtiar, *Biotechnol. Lett.* **2016**, 38, 1–10.
- [18] T. Lammers, F. Kiessling, W. E. Hennink, G. Storm, *J. Control. Release* **2012**, 161, 175–187.
- [19] S. Wang, P. Huang, X. Chen, *Adv. Mater.* **2016**, 28, 7340–7364.
- [20] J. Fang, H. Nakamura, H. Maeda, *Adv. Drug Deliv. Rev.* **2011**, 63, 136–151.
- [21] H. Nakamura, F. Jun, H. Maeda, **2015**, 53–64.
- [22] J. Zhang, Z.-F. Yuan, Y. Wang, W.-H. Chen, G.-F. Luo, S.-X. Cheng, R.-X. Zhuo, X.-Z. Zhang, *J. Am. Chem. Soc.* **2013**, 135, 5068–73.
- [23] K. Husmann, R. Muff, M. E. Bolander, G. Sarkar, W. Born, B. Fuchs, *Mol. Carcinog.* **2008**, 47, 66–73.
- [24] G. Bonzi, S. Salmaso, A. Scamparin, A. Eldar-Boock, R. Satchi-Fainaro, P. Caliceti, *Bioconjug. Chem.* **2015**, 26, 489–501.

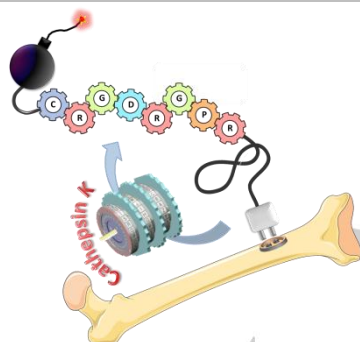
- [25] H. Uludag, J. Yang, *Biotechnol. Prog.* **2002**, *18*, 604–611.
- [26] S. Kunjachan, R. Pola, F. Gremse, B. Theek, J. Ehling, D. Moeckel, B. Hermanns-sachweh, M. Pechar, K. Ulbrich, W. E. Hennink, et al., *Nano Lett.* **2014**, *14*, 972–981.
- [27] D. J. Burkhart, B. T. Kalet, M. P. Coleman, G. C. Post, T. H. Koch, *Mol. Cancer Ther.* **2004**, *3*, 1593–1604.
- [28] W. Jahnke, C. Henry, *ChemMedChem* **2010**, *5*, 770–6.
- [29] S. Zitzmann, V. Ehemann, M. Schwab, *Cancer Res.* **2002**, *62*, 5139–5143.
- [30] Y. Choe, F. Leonetti, D. C. Greenbaum, F. Lecaille, M. Bogoy, D. Brömme, J. A. Ellman, C. S. Craik, *J. Biol. Chem.* **2006**, *281*, 12824–32.
- [31] S. R. Wilson, C. Peters, P. Saftig, D. Brömme, *J. Biol. Chem.* **2009**, *284*, 2584–92.
- [32] E. Vlashi, L. E. Kelderhouse, J. E. Sturgis, P. S. Low, **2013**, 8573–8582.
- [33] X. Duan, S.-F. Jia, Z. Zhou, R. R. Langley, M. F. Bolontrade, E. S. Kleinerman, *Clin. Exp. Metastasis* **2004**, *21*, 747–53.
- [34] H. Zhu, H. Cai, M. Tang, J. Tang, *Clin. Transl. Oncol.* **2014**, *16*, 732–738.
- [35] J. D. Lamplot, S. Denduluri, J. Qin, R. Li, X. Liu, H. Zhang, X. Chen, N. Wang, A. Pratt, W. Shui, et al., *Curr Cancer Ther Rev* **2016**, *9*, 55–77.

## Layout 1: Bony &amp; Hide

A double sequential encrypted targeting system able to recognize bone tissue in the first place and then, osteosarcoma cells through an cascade process activated by cathepsin K present in the diseased tissue.

## COMMUNICATION

A double sequential encrypted targeting system able to recognize bone tissue in the first place and then, osteosarcoma cells through an cascade process activated by cathepsin K present in the diseased tissue.



Gonzalo Villaverde, Valentina Nairi, Alejandro Baeza,\* and María Vallet-Regí.\*

Page No. – Page No.

Title Double sequential encrypted targeting sequence: A new concept for bone cancer treatment.